

## Multigene Family Encoding 3',5'-Cyclic-GMP-Dependent Protein Kinases in *Paramecium tetraurelia* Cells

Roland Kissmehl,<sup>1\*</sup> Tim P. Krüger,<sup>1</sup> Tilman Treptau,<sup>1</sup> Marine Froissard,<sup>2</sup>  
and Helmut Plattner<sup>1</sup>

Department of Biology, University of Konstanz, 78457 Konstanz, Germany,<sup>1</sup> and Centre de Génétique Moléculaire, CNRS, Avenue de la Terrasse, 91198 Gif-sur-Yvette, France<sup>2</sup>

Received 9 June 2005/Accepted 1 November 2005

**In the ciliate *Paramecium tetraurelia*, 3',5'-cyclic GMP (cGMP) is one of the second messengers involved in several signal transduction pathways. The enzymes for its production and degradation are well established for these cells, whereas less is known about the potential effector proteins. On the basis of a current *Paramecium* genome project, we have identified a multigene family with at least 35 members, all of which encode cGMP-dependent protein kinases (PKGs). They can be classified into 16 subfamilies with several members each. Two of the genes, *PKG1-1* and *PKG2-1*, were analyzed in more detail after molecular cloning. They encode monomeric enzymes of 770 and 819 amino acids, respectively, whose overall domain organization resembles that in higher eukaryotes. The enzymes contain a regulatory domain of two tandem cyclic nucleotide-binding sites flanked by an amino-terminal region for intracellular localization and a catalytic domain with highly conserved regions for ATP binding and catalysis. However, some *Paramecium* PKGs show a different structure. In Western blots, PKGs are detected both as cytosolic and as structure-bound forms. Immunofluorescence labeling shows enrichment in the cell cortex, notably around the dense-core secretory vesicles (trichocysts), as well as in cilia. Immunogold electron microscopy analysis reveals consistent labeling of ciliary membranes, of the membrane complex composed of cell membrane and cortical Ca<sup>2+</sup> stores, and of regions adjacent to ciliary basal bodies, trichocysts, and trafficking vesicles. Since PKGs (re)phosphorylate the exocytosis-sensitive phosphoprotein pp63/pf upon stimulation, the role of PKGs during stimulated exocytosis is discussed, in addition to a role in ciliary beat regulation.**

In eukaryotic cells, 3',5'-cyclic GMP (cGMP) is one of the second messengers participating in signal transduction pathways. Its significance has been only partially elucidated. Three effector activities are currently discussed (48, 77), namely, (i) cGMP-induced activation of ion channels, (ii) cGMP-sensitive phosphodiesterase (PD) activity, and (iii) Ser/Thr-specific cGMP-dependent protein kinase (PKG) activity. PKGs are found not only in metazoans of different phyla (48, 60) but also in flowering plants (73) and lower eukaryotes (16, 23). The metazoan PKGs can be divided into two types, a soluble type I form with several splice forms (58, 66, 83) and a single membrane-bound type II form (33, 76). Unlike mammalian and invertebrate PKGs, which are typically homodimers, the protozoan PKGs known so far are all monomeric proteins (16, 23, 55, 80). The multiple interactions of PKGs with other signaling systems (77) are particularly intriguing. Signaling via PKGs presupposes the occurrence of a guanylate cyclase (GC) and termination by PD activity.

Among potential signaling components, the following are known to occur in the ciliate *Paramecium*: a Ca<sup>2+</sup>-dependent GC (47, 67), PD (68), and a PKG (53). The broad spectrum of cellular activities governed or modulated by PKGs led us to identify the corresponding genes.

Our approach is based on the recent availability of an indexed genomic library (34), on an international *Paramecium*

genome project (13, 72), and on sequencing data from either a 1-megabase chromosome (86) or from an ongoing genome project provided by Genoscope (France). We were surprised by the occurrence of an extensive family of PKG genes in *Paramecium*, in contrast to the global description of PKG activity in cilia and whole-cell bodies (53) without any further differentiation.

The large number of genes we found may reflect the broad range of activities observed with or related to cGMP formation in *Paramecium*. This includes depolarization-induced ciliary reversal (84), circadian rhythms (25), and exocytosis, particularly with regard to rephosphorylation of pp63/pf (parafusin), an exocytosis-sensitive phosphoprotein of 63 kDa (36, 43, 54). The recent suggestion of a potential role of PKG includes actin filament reorganization and/or intracellular trafficking in mammalian cells (32). For *Paramecium*, this may turn out to be important with regard to extensive membrane trafficking (62).

In summary, the broad spectrum of PKG genes we now find may facilitate further elucidation of PKGs in widely different functions of *Paramecium* cells. Moreover, a comparison with pathogenic relatives of *Paramecium* in the phylum Alveolata, i.e., *Toxoplasma*, *Plasmodium*, *Eimeria*, etc. (Apicomplexa), revealed interesting observations.

### MATERIALS AND METHODS

**Cell cultures and cell fractionation.** The wild-type strains of *Paramecium tetraurelia* used were stock strains 7S and d4-2, derived from stock strain 51S (71). Cells were cultivated either in a bacterized medium or, for subcellular fractionation, in an axenic medium as previously described (40). Whole-cell homogenates were prepared in phase buffer (20 mM Tris-maleate, 20 mM NaOH, 20

\* Corresponding author. Mailing address: Department of Biology, University of Konstanz, P.O. Box 5560, 78457 Konstanz, Germany. Phone: 49-7531-88-3712. Fax: 49-7531-88-2245. E-mail: roland.kissmehl@uni-konstanz.de.

mM NaCl, 250 mM sucrose, pH 7.0) by ~100 hand strokes in a glass homogenizer equipped with a Teflon pestle. Soluble and particulate fractions were separated by centrifugation at  $100,000 \times g$  for 60 min at 4°C. Cell surface complexes (cortices) were prepared according to the method of Lumpert et al. (49), and cilia were purified by differential centrifugation after applying the  $Mn^{2+}$ -shock method (57). A protease inhibitor cocktail containing 15  $\mu$ M pepstatin A, 100 mU/ml aprotinin, 100  $\mu$ M leupeptin, 0.26 mM *N*-*p*-tosyl-L-arginine methyl ester, 28  $\mu$ M E64, and 0.2 mM Pefabloc SC was used throughout.

**PCRs with genomic DNA.** For PCR, total wild-type DNA was prepared from log-phase d4-2 cell cultures as described previously (28). For *PKG1-1*, the probe consisted of a 474-bp PCR amplification product made with the following primers (MWG-Biotech, Ebersberg, Germany): 5' oligonucleotide 1, 5'-CAAGTGA CCAAACAAGGC-3'; and 3' oligonucleotide 2, 5'-GATTGATTTTTCGTTTT TGTTTC-3'. For *PKG2-1*, the probe was a 514-bp PCR amplification product created with the following two primers: 5' oligonucleotide 3, 5'-TTCAATAAT ATTATGAGATGGAG-3'; and 3' oligonucleotide 4, 5'-ACCTTTTTTGTTTC TTTGTGC-3'. Each PCR mixture (50  $\mu$ l) contained 20 ng of DNA, a 200 nM concentration of each primer, a 0.2 mM concentration of each deoxynucleoside triphosphate, and 1  $\mu$ l of Advantage 2 DNA polymerase (Clontech Laboratories, Inc., Heidelberg, Germany). Reactions were carried out for 1 cycle of denaturation (1 min, 95°C) and 35 cycles of denaturation (30 s, 95°C), annealing (45 s, 46°C), and extension (60 s, 68°C), with a final extension step (5 min, 68°C).

Screening of a genomic  $\lambda$ ZAPII library of EcoRI-digested macronucleic DNA from *P. tetraurelia* ( $5 \times 10^6$  primary plaques) was performed by using a PCR-based strategy (4) in which the universal T3 primer was combined with each of three nested *PKG2-1*-specific 3' oligonucleotides, oligonucleotides 5 to 7 (3' oligonucleotide 5, 5'-ACCTTTTTTGTTTC TTTGTGC-3'; 3' oligonucleotide 6, 5'-CTTTTGAGTGAATCTTGAGG-3'; and 3' oligonucleotide 7, 5'-TCTAC ATCCTCTCCTCCTC-3'). Following one denaturation step (95°C, 1 min), 39 cycles of amplification (30 s at 95°C, 45 s at 56°C, and 60 s at 68°C) and a final elongation step of 3 min at 68°C were carried out. For three consecutive PCRs, the resulting PCR product (~50 ng) was used as a new template for the subsequent reaction with the nested primer. *PKG*-specific PCR products were cloned into the plasmid pCR2.1 by using a TOPO-TA cloning kit (Invitrogen, Karlsruhe, Germany) according to the manufacturer's instructions. After transformation into *Escherichia coli* (DH5 $\alpha$  or TOP10F' cells), positive clones were sequenced as described below.

**PCRs with cDNAs.** The open reading frames (ORFs) of *PKG1-1* and *PKG2-1* were amplified by reverse transcriptase PCR (RT-PCR), using total RNA prepared according to the protocol described by Haynes et al. (29). RT-PCR was performed in a programmable T3 thermocycler (Biometra, Göttingen, Germany), using oligonucleotide 8 and PowerScript reverse transcriptase (Clontech Labs) for first-strand cDNA synthesis (3' oligonucleotide 8, 5'-AACTGGAAG AATTCGCGGCCGCGAATTTTTTTTTTTTTT-3'). The subsequent PCR (50  $\mu$ l) was performed with Advantage 2 cDNA polymerase mix (Clontech Labs), using either the *PKG1-1*-specific primers 9 and 10 (5' oligonucleotide 9, 5'-GATCAGATGATTCCTGGGT-3'; and 3' oligonucleotide 10, 5'-TTCAAAAAG TCTTAATCCAGTC-3') or the *PKG2-1*-specific primers 11 and 12 (5' oligonucleotide 11, 5'-ATCTTTGAAAAGTGCCAGTA-3'; and 3' oligonucleotide 12, 5'-GTTCTGTATTATATTCAAAAAGTC-3'), with the last two containing artificial restriction sites added at their 5' ends (SpeI and XhoI, respectively). Amplifications were performed with 1 cycle of denaturation (95°C, 1 min) and 39 cycles of denaturation (95°C, 30 s), annealing (58°C, 45 s), and extension (68°C, 3 min), followed by a final extension step at 68°C for 5 min. PCR products were cloned and sequenced as described below.

**Sequencing.** Sequencing was done by the MWG Biotech (Ebersberg, Germany) custom sequencing service. DNA sequences were aligned with CLUSTAL W integrated into the DNASTAR Lasergene software package (Madison, WI).

**Annotation of further *PKG* genes.** In order to identify further paralogs of *PKGs*, the developing *Paramecium* database (<http://paramecium.cgm.cnrs-gif.fr/ptblast/>) was screened by using the nucleotide and amino acid sequences of *PKG1-1* and *PKG2-1*. Positive hits were further analyzed by performing BLAST searches at the NCBI database (2). Conserved motif searching was performed with either PROSITE (6) or BLAST-RPS, using pfam entries of the corresponding CDD database (52).

**Southern hybridization.** Radioactive probes were synthesized by [ $\alpha$ - $^{32}$ P]dATP incorporation using a random primer labeling system (Gibco-BRL, Cergy-Pontoise, France) according to the supplier's protocol. Nonradioactive probes were made using digoxigenin-labeled nucleotides (Roche, Indianapolis, Ind.). Hybridizations with an indexed library of *Paramecium* macronuclear DNAs were carried out as described by Keller and Cohen (34).

**Expression of a *Paramecium* *PKG1-1*-specific peptide in *E. coli*.** For heterologous expression of a *PKG*-specific peptide, we selected the amino acid sequence

of *PKG1-1* (accession number AJ550184). After changing all deviating *Paramecium* glutamine codons (TAA and TAG) to universal glutamine codons (CAA and CAG) by PCR methods (15), the coding region for F266 to Q445 of *Paramecium* *PKG1-1* was cloned into the XhoI/BamHI restriction sites of the pET16b expression vector of the Novagen pET system (Madison, WI), which adds a 24-amino-acid peptide at the N terminus of the selected sequence, including a His<sub>10</sub> tag for purification of the recombinant peptide.

**Purification of a recombinant *PKG1-1* peptide and preparation of polyclonal antibodies.** The recombinant *PKG1-1* peptide, *PKG1-1*<sub>F266-Q445</sub>, was purified by affinity chromatography on Ni<sup>2+</sup>-nitrilotriacetate-agarose under denaturing conditions, as recommended by the manufacturer (Novagen), and was used for immunization of rabbits. After several boosts, positive sera were taken and affinity purified by two subsequent chromatography steps, as described in detail by Kissmehl et al. (40).

**SDS-polyacrylamide gel electrophoresis and immunoblotting.** Protein samples were denatured by boiling for 3 min in a sample buffer (0.4 M Tris-HCl, 1% sodium dodecyl sulfate [SDS], 0.5% dithiothreitol, 20% glycerol, pH 8.0) without subsequent alkylation and then subjected to electrophoresis in 10% SDS-polyacrylamide gels using a discontinuous buffer system as described previously (37). The replicas were electroblotted onto nitrocellulose membranes, and immunobinding was carried out as described previously (40), using affinity-purified antibodies (Abs) against *PKG1-1*. Bound Abs were detected with a corresponding peroxidase-conjugated secondary Ab (anti-rabbit immunoglobulin G), using the Amersham enhanced chemiluminescence (ECL) detection system.

**Isolation of *PKGs* and phosphorylation studies.** The isolation of *PKGs* was performed according to a protocol described by Kissmehl et al. (36). Standard assays for *PKG* activity were performed with histone II-S, an established in vitro substrate for *PKGs* (36). Phosphorylation of recombinant pp63/pf (26) was accomplished in a reaction volume of 45  $\mu$ l containing 20 mM triethanolamine-HCl, 240 mM NaCl, 10% glycerol in the presence of 5 mM MgCl<sub>2</sub>, 0.12 mM ATP, [ $\gamma$ - $^{32}$ P]ATP (185 MBq/ $\mu$ mol), 3  $\mu$ g of recombinant pp63/pf, with or without cGMP (0.15  $\mu$ M), 8-chlorophenylthio (pCPT)-cGMP (0.15  $\mu$ M), and the *PKG* fraction (1.275  $\mu$ g). At the end of the incubation (20 min at 20°C), 25- $\mu$ l aliquots were subjected to SDS-polyacrylamide gel electrophoresis and processed for autoradiography.

**Immuno-LM and -EM analysis.** For immuno-light microscopy (immuno-LM), cells were prepared basically as previously described (39), except that 1% Triton X-100 was replaced by 0.5% digitonin as a permeabilization agent. After exposure to affinity-purified anti-*PKG1-1* Abs and fluorescein isothiocyanate-conjugated anti-rabbit Abs (Sigma-Aldrich, St. Louis, MO), both diluted 1:100 in phosphate-buffered saline plus 1% bovine serum albumin, fluorescence staining was analyzed either by conventional LM or by confocal laser scanning microscopy, as previously described (40). Images acquired with LSM 510 software were processed with Photoshop software (Adobe Systems, San Jose, CA). For immuno-electron microscopy (immuno-EM) analysis, samples were prepared as described previously (40). Primary anti-*PKG* Abs from rabbits were detected with protein A-gold conjugates with a 5-nm diameter (Au<sub>5 nm</sub>) on ultrathin sections which were "stained" with uranyl acetate.

## RESULTS

On the basis of three independently initiated *Paramecium* genome projects, we were able to identify a *PKG* multigene family with at least 35 members. These projects included a pilot sequencing project (13, 72), the sequencing of a macronucleic 1-megabase chromosome (86), and the current genome project initiated by the GDRE (Groupement de Recherches Européen), coordinated by Jean Cohen and Linda Sperling (CNRS, France) in collaboration with Genoscope (Evry, France). *PKGs* of *Paramecium* can be classified into 16 subfamilies with several members each, two of which, *PKG1-1* and *PKG2-1*, were analyzed in more detail after their molecular cloning.

***PKG 1* subfamily.** First, a partial sequence of a *PKG* encoding protein was found in the pilot genome project of *Paramecium* (13, 72). Sequencing of the corresponding clone, 7i7, resulted in the identification of the 3' end of this gene. In order to obtain the missing 5' end, we took advantage of an indexed

genomic library, which we analyzed in two subsequent hybridization steps (34) by using a specific probe designed from the 7i7 sequence (Fig. 1A, top). Besides clone 7i7, another three clones were then retrieved, namely, 8g1, 8n17, and 114d24. All three contain the missing 5' sequence information of this gene, called *PKG1-1* (accession number AJ550184).

The *PKG1-1* gene, consisting of 2,489 bp, encodes a protein of 770 amino acids with a calculated molecular mass of 89.3 kDa (Table 1). A comparison of the genomic sequence with the cDNA equivalent revealed that the gene is expressed and that the ORF is interrupted by seven short introns (Fig. 1A, top), which all display the characteristics of *Paramecium* introns (65, 72), i.e., bordering by 5'-GT and AG-3' and a size of 21 to 30 nucleotides.

The overall structure of the gene product resembles that of proteins in higher eukaryotes (60). PKG1-1 is composed of three putative functional domains, i.e., a catalytic domain which would catalyze the transfer of  $\gamma$ -phosphate from ATP to a serine/threonine residue of a substrate protein, a regulatory domain with two tandem cyclic nucleotide-binding sites, and an amino-terminal domain (Fig. 1A, bottom). It does not contain a transmembrane domain (Fig. 1B), but there are several putative N-myristoylation sites (Fig. 1C), one of which occurs at the amino terminus, as is typical for type II PKGs (78). This would allow the enzyme to be localized not only in the cytosolic fraction but also in particulate fractions. In contrast to PKGs from higher eukaryotes, the amino terminus of PKG1-1 does not contain a hydrophobic leucine/isoleucine zipper motif, which is required for dimerization (5, 46), suggesting its occurrence as a monomeric enzyme in *P. tetraurelia*. There are also no autophosphorylation sites at the amino terminus, which are known to enhance the basal activity of the enzyme as well as to increase the affinity of type I PKGs for cAMP (45, 70). They normally are located in close proximity to a highly conserved region at the amino terminus. This region interacts with the catalytic center and inhibits enzyme activity in the absence of bound cGMP (35). However, in PKG1-1, such a pseudosubstrate sequence is either absent or not very well conserved.

The regulatory domain consists of two highly conserved cyclic nucleotide-binding domains of ~120 amino acids each (69, 82), both of which are present in PKG1-1 and display remarkable sequence identity (Fig. 1D). From the analysis of the prokaryotic CAP gene, it is known that such a domain is composed of a  $\beta$ -barrel formed by eight antiparallel  $\beta$ -sheets ( $\beta$ 1 to 8) and three flanking  $\alpha$ -helices (81). There are several invariant amino acids, three of which are glycine residues considered essential for maintenance of the structural integrity of the beta-barrel. Two of them are located within  $\beta$ 2 and  $\beta$ 3 (signature 1), whereas the third conserved glycine occurs in the second signature (within  $\beta$ 6 and  $\beta$ 7) as part of the consensus sequence F-G-E, which forms a conserved binding pocket for the ribose phosphate moiety. This signature also occurs in PKG1-1 (Fig. 1D), where it contains another invariant amino acid, an arginine residue, which chelates the cyclic phosphate diester as part of the conserved sequence R-S/T/A-A. However, the two cGMP-binding domains also differ remarkably from each other and therefore may have different biochemical properties. This has been reported for mammalian PKGs, where only the domain located close to the amino terminus has

been identified as having slow dissociation characteristics and a high binding affinity (64).

The boundary between the putative catalytic domain and the second cGMP-binding domain is located seven residues upstream from the first glycine of the highly conserved consensus motif (G-X-G-X-X-G-X-V/A) for ATP binding (Fig. 1E), where a hydrophobic residue (phenylalanine) is usually found (24). Another motif, termed the catalytic loop, contains an aspartate (D580) as the putative base accepting the proton from the attacking substrate hydroxyl group during the phosphate transfer reaction. This motif is also present in PKG1-1 (Fig. 1E). The lysine at position 582 of this loop may help to facilitate the phosphor transfer by neutralizing the negative charge of the  $\gamma$ -phosphate during transfer. PKG1-1 also contains a putative activation loop close to the active center (Fig. 1E), in which a phosphothreonine would be required for a catalytically active enzyme (18). Beyond that, there are several highly conserved amino acids in the C-terminal part of the catalytic domain of PKG1-1, including those forming the motif H-X-W-F, which defines the boundary of the carboxyl-terminal domain (Fig. 1E). In mammalian PKGs, the latter domain is thought to contribute to substrate recognition (60).

The overall identities of PKG1-1 with type I or type II PKGs from higher eukaryotes range, on the amino acid level, from 20.0% to 22.7% (Table 2). However, the overall identity to PKGs from the more related Apicomplexan group is much higher (~33%), although the PKGs are not classified as one or the other of the two subtypes occurring in metazoans (16, 23).

By BLAST searching with the complete sequence of *PKG1-1* in the *Paramecium* database, another three members of this PKG 1 subfamily were identified, which have been grouped together not only due to their close relationship but also due to the same number and position of introns interrupting their ORFs (Table 1). Therefore, they were designated *PKG1-2* to *PKG1-4*. They all encode proteins of 770 amino acids, with calculated molecular masses ranging from 88.8 to 89.5 kDa (Table 1). Their identities to PKG1-1 vary between ~74% and 83% at the nucleotide sequence level and between ~84 and 89% at the protein sequence level (Table 1). Sequence alignments with PKG proteins from other species revealed similar values for each of the new members of this *Paramecium* subfamily to those found for PKG1-1, showing highest similarities to PKGs from Apicomplexan organisms (Table 2).

**PKG 2 subfamily.** In the pilot genome project of *Paramecium* (13, 72), a second partial sequence was found resembling PKGs. In order to obtain the full gene information, we first completed sequencing of the corresponding clone, 22C23, by which we obtained the 3' end. For the missing 5' end, we performed Southern hybridizations in which the indexed genomic library (34) was probed with a PCR fragment located in the middle of the gene (Fig. 1G, top). However, none of the clones obtained contained the missing 5' sequence information for this PKG gene. We finally were successful by screening a genomic  $\lambda$ ZAPII library of EcoRI-digested macronucleic DNA from *P. tetraurelia* with a nested PCR technique (4). The complete gene was called *PKG2-1* (accession number AJ550185). With its 2,642 bp, it encodes a soluble enzyme of 819 amino acids with a calculated molecular mass of 94.0 kDa (Fig. 1G; Table 1). RT-PCR analysis revealed that *PKG2-1* is expressed and that its ORF is interrupted by seven short in-

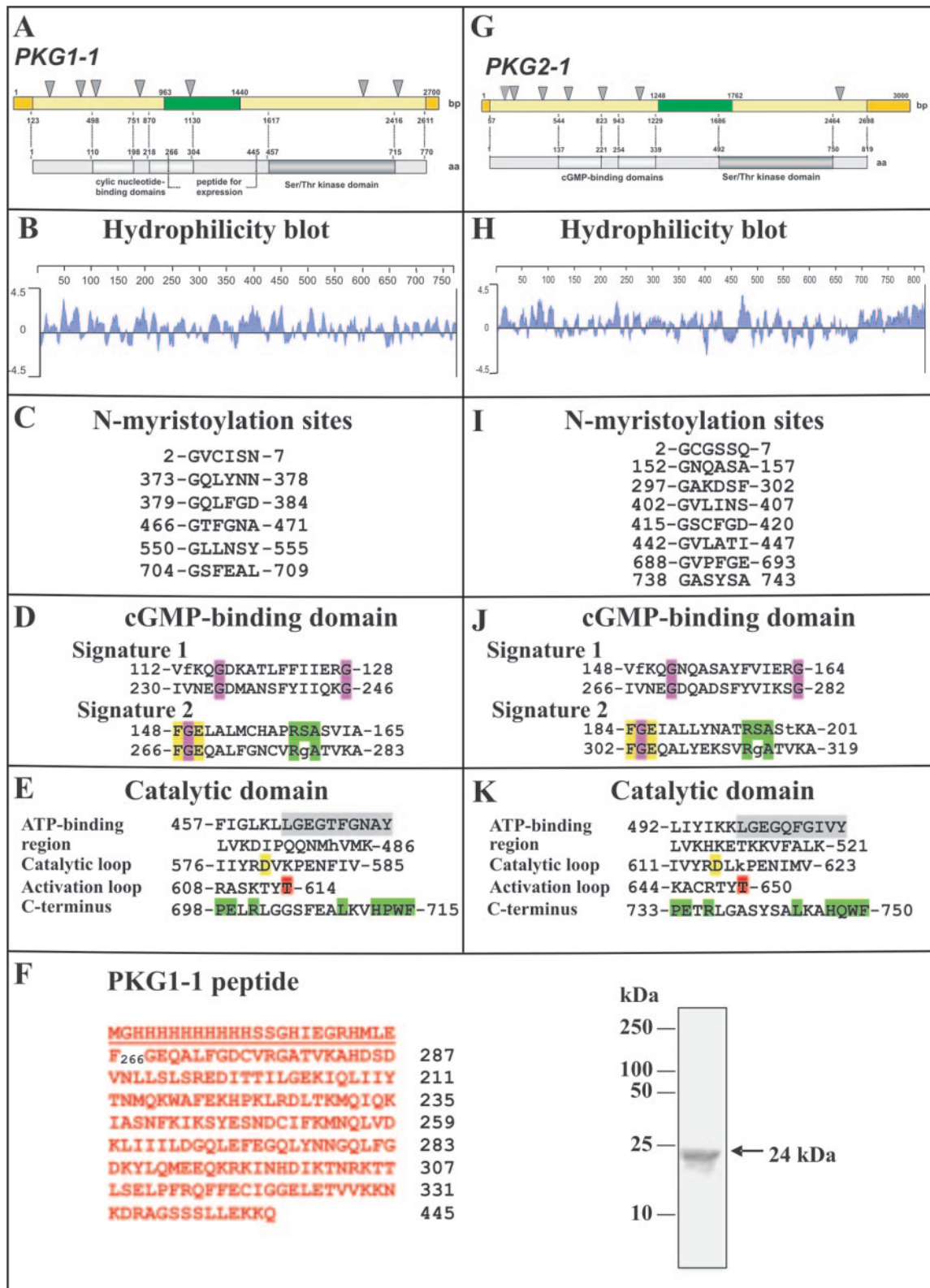


FIG. 1. Characteristics of cGMP-dependent protein kinases PKG1-1 and PKG2-1 from *Paramecium tetraurelia*. (A and G) Schematic diagrams of PKG1-1 (A) and PKG2-1 (G) at the nucleotide (top) and amino acid (bottom) levels. (Top) Positions of introns are indicated (gray arrowheads). Orange areas are untranslated regions at the 5' and 3' ends of the coding sequence. The region used as a probe is labeled in green. The numbers indicated represent the nucleotide positions within the genomic versions of the two genes. (Bottom) Characteristic features such as the Ser/Thr kinase domain and the two cyclic nucleotide-binding domains are labeled with different shades of gray. The region of PKG1-1 used for raising Abs is shown in more detail in panel F. (B and H) Hydrophilicity plots according to the algorithms of Kyte and Doolittle

TABLE 1. Characteristics of PKG genes in *Paramecium tetraurelia*

Gene	Accession no.	Characteristic of DNA				Characteristic of protein			
		Length (bp)	ORF (bp)	Introns ( <i>n</i> )	Identity <sup>a</sup> (%)	Length (aa)	Size (kDa)	Identity <sup>a</sup> (%)	Identity <sup>a,b</sup> (%)
<i>PKG1-1</i>	AJ550184	2,489	2,313	7	100	770	89.3	100	100
<i>PKG1-2</i>	CR855963	2,481	2,313	7	83.4	770	89.5	89.2	89.2
<i>PKG1-3</i>	CR855962	2,498	2,313	7	75.2	770	88.8	85.0	85.0
<i>PKG1-4</i>	CR855961	2,498	2,313	7	74.1	770	89.3	83.8	83.8
<i>PKG2-1</i>	AJ550185	2,642	2,460	7	100	819	94.0	100	45.5
<i>PKG2-2</i>	CR855951	2,643	2,460	7	86.7	819	94.0	92.9	45.0
<i>PKG3-1</i>	CR855950	2,699	2,478	9	100	825	94.8	100	42.9
<i>PKG3-2</i>	CR855949	2,697	2,478	9	91.2	825	94.5	97.0	42.9
<i>PKG4-1</i>	CR855948	2,556	2,373	7	100	790	91.9	100	44.2
<i>PKG4-2</i>	CR855947	2,556	2,373	7	87.6	790	91.9	86.9	44.5
<i>PKG5-1</i>	CR855946	2,638	2,442	8	100	813	93.3	100	46.7
<i>PKG5-2</i>	CR548612	2,645	2,442	8	88.1	813	93.1	94.7	46.4
<i>PKG5-3</i>	CR855945	2,627	2,424	8	79.8	807	92.7	91.5	47.1
<i>PKG5-4</i>	CR855944	2,623	2,424	8	79.4	770	92.5	90.2	47.0
<i>PKG6-1</i>	CR856019	2,617	2,448	7	100	815	94.2	100	47.3
<i>PKG6-2</i>	CR855942	2,621	2,448	7	89.9	815	94.1	96.8	47.6
<i>PKG7-1</i>	CR855941	2,623	2,448	7	100	815	93.9	100	44.1
<i>PKG8-1</i>	CR855940	2,491	2,388	5	100	795	91.3	100	35.5
<i>PKG8-2</i>	CR855939	2,490	2,388	5	85.2	795	91.4	91.9	35.0
<i>PKG9-1</i>	CR855938	2,472	2,343	5	100	780	88.6	100	36.4
<i>PKG9-2</i>	CR855937	2,477	2,343	5	88.2	780	88.6	94.1	36.1
<i>PKG9-3</i>	CR855936	2,459	2,337	5	78.8	778	88.6	89.4	35.5
<i>PKG9-4</i>	CR855935	2,465	2,340	5	77.4	779	88.7	86.6	34.4
<i>PKG10-1</i>	CR855960	2,405	2,244	7	100	747	85.7	100	35.1
<i>PKG10-2</i>	CR855959	2,410	2,244	7	86.6	747	85.8	91.6	35.7
<i>PKG11-1</i>	CR855958	2,637	2,325	12	100	774	89.3	100	41.1
<i>PKG11-2</i>	CR855957	2,635	2,325	12	89.2	774	89.2	98.5	41.4
<i>PKG11-3</i>	CR855984	2,635	2,328	12	80.9	775	89.2	97.2	41.1
<i>PKG12-1</i>	CR855956	2,570	2,292	11	100	763	88.7	100	37.5
<i>PKG13-1</i>	CR855955	2,638	2,454	7	100	817	93.8	100	46.6
<i>PKG13-2</i>	CR855983	2,645	2,454	7	75.6	817	93.9	86.1	46.0
<i>PKG13-3</i>	CR855982	2,646	2,457	7	75.6	818	93.9	85.1	45.5
<i>PKG14-1</i>	CR855954	2,575	2,433	6	100	810	93.3	100	41.5
<i>PKG15-1</i>	CR855953	2,172	2,079	4	100	692	80.8	100	28.3
<i>PKG16-1</i>	CR855952	1,989	1,989	0	100	662	77.1	100	22.7

<sup>a</sup> Sequences were aligned by the Clustal W method.

<sup>b</sup> Numbers are referred to the amino acid sequence of PKG1-1.

trons (Fig. 1G). The overall domain structure closely resembles that of PKG1-1 (Fig. 1H to K). However, there are several insertions in the amino-terminal region as well as at the carboxy terminus of the enzyme. In metazoans, such regions are known to be involved in the dimerization of homologous subunits, autoinhibition of the catalytic domain in the absence of cGMP, and substrate recognition (60). Therefore, the variations we observed may entail different functional consequences to be analyzed in future studies.

By BLAST searching with the complete sequence of *PKG2-1* in the *Paramecium* database, another member of this PKG 2 subfamily has been identified (Table 1). This gene, designated *PKG2-2*, encodes a protein of 819 amino acids which is >92% identical to *PKG2-1* and >45% identical to members of the

PKG 1 subfamily (Table 1). Sequence alignments with PKG proteins from other species show the highest similarity to PKGs from the Apicomplexan group, as observed also for the members of the PKG 1 subfamily (Table 2).

**Further PKG subfamilies.** BLAST results from the *Paramecium* database revealed the presence of further PKG-encoding genes in the macronucleic genome, which have been divided into subfamilies 3 to 16 according to their characteristic gene and protein structures (Table 1). Within a given subfamily, the members differ by only up to 26% at the nucleotide level and even less ( $\leq 15\%$ ) at the amino acid level. Their ORFs are interrupted by the same numbers of introns, all located at corresponding positions (Table 1). However, between the various subfamilies, the numbers and positions of introns are

(44). The positions and sequences of putative N-myristoylation sites (C and I) as well as of the two signatures within each cyclic nucleotide-binding domain (D and J) are shown. Deviations from the consensus are shown with lowercase letters. Magenta, highly conserved amino acids, e.g., for the maintenance of the structural integrity of the  $\beta$ -barrel; yellow, binding sites for the ribose phosphate moieties; green, binding site for the guanine base. (E and K) Sequences important for catalysis include the ATP-binding regions with a consensus for ATP binding (gray), the loop with the catalytic aspartate at position 580 or 615 (yellow), the activation loops with a threonine for putative autophosphorylation at positions 614 and 650 (red), and the C-terminal part of the catalytic domains with some invariant residues (green). (F) The *PKG1-1* peptide containing a His tag at the N terminus (underlined) consists of 203 amino acids (left). After heterologous expression in *E. coli*, it is visible predominantly as a 24-kDa band on a silver-stained SDS-polyacrylamide gel (right).

TABLE 2. Multiple alignment of PKGs from different species<sup>a</sup>

PKG	<i>T. gondii</i> PKG % identity	<i>P. falciparum</i> PKG % identity	<i>O. sativa</i> PKG1 % identity	<i>H. sapiens</i> PKG1 % identity	<i>G. gallus</i> PKG2 % identity	<i>M. musculus</i> PKG2 % identity
PKG1-1	32.9	32.3	20.0	23.6	22.7	22.3
PKG1-2	32.2	30.7	19.5	23.1	22.6	22.4
PKG1-3	32.6	30.5	19.7	23.2	21.8	21.9
PKG1-4	32.6	31.0	19.7	23.1	21.8	22.2
PKG2-1	34.3	32.1	17.4	20.9	21.8	21.1
PKG2-2	34.0	31.8	17.3	20.7	21.8	21.0
PKG3-1	35.1	33.3	17.9	21.2	22.0	21.5
PKG3-2	35.4	33.7	17.7	21.3	21.7	21.5
PKG4-1	31.6	30.8	18.1	19.2	20.9	20.0
PKG4-2	32.1	31.4	18.1	19.5	20.6	19.8
PKG5-1	31.2	30.0	18.9	19.5	20.9	21.1
PKG5-2	31.3	30.0	18.4	19.4	20.5	20.8
PKG5-3	32.1	30.9	19.1	19.6	20.7	20.9
PKG5-4	32.8	31.1	19.1	19.4	20.5	20.7
PKG6-1	32.4	30.8	18.4	20.5	19.6	19.6
PKG6-2	32.6	30.8	18.0	20.7	19.9	19.9
PKG7-1	30.6	29.4	17.3	19.9	19.5	20.1
PKG8-1	33.9	31.2	17.3	21.4	21.2	22.0
PKG8-2	33.7	31.2	17.8	20.7	21.7	22.1
PKG9-1	33.3	30.9	17.7	20.7	22.7	22.5
PKG9-2	33.0	30.6	18.1	20.5	22.5	22.4
PKG9-3	32.5	30.7	18.4	21.1	23.2	23.6
PKG9-4	32.9	30.6	18.2	20.3	22.6	22.9
PKG10-1	34.0	34.9	18.0	21.1	23.4	23.1
PKG10-2	34.0	34.4	18.3	21.3	22.6	22.2
PKG11-1	33.5	33.2	19.5	21.2	21.0	22.5
PKG11-2	33.7	33.7	19.4	21.2	21.2	22.6
PKG11-3	33.9	33.6	19.8	20.7	21.1	22.6
PKG12-1	32.2	31.4	19.5	21.9	21.3	23.3
PKG13-1	33.0	29.8	18.9	21.3	20.3	21.1
PKG13-2	31.5	29.7	19.2	22.1	20.9	21.6
PKG13-3	31.3	29.4	19.0	21.4	20.5	21.4
PKG14-1	34.2	32.2	18.7	21.5	22.3	22.9
PKG15-1	26.6	27.1	15.6	17.7	19.9	19.3
PKG16-1	25.0	25.3	15.4	16.4	19.0	18.4

<sup>a</sup> PKG protein sequences from *Paramecium tetraurelia* (PKG1-1 to PKG16-1), *Toxoplasma gondii* (AAM27174), *Plasmodium falciparum* (AAM22644), *Oryza sativa* (BAD22406), *Homo sapiens* (BAA08297), *Mus musculus* (AAA02572), and *Gallus gallus* (XP\_426309) were aligned using the Clustal W program.

extremely variable, with their number ranging from 0 to 12 (Table 1). This heterogeneity is also reflected by a phylogenetic analysis which suggests that all *Paramecium* PKGs may be derived from a common ancestral intron-free gene (Fig. 2). The analysis also reveals that several duplication events might be the reason for the occurrence of the numerous PKG paralogs in *P. tetraurelia*, including a recent duplication of the whole genome (L. Sperling and J. Cohen, personal communication) that resulted in a second, closely related paralog within most of the subfamilies (Fig. 2; Table 1). Remarkably, similarity values between the subfamilies are still high, ranging from 35 to 45% on average when referred to PKG1-1 (Table 1). Compared with PKGs from other species, the sequence alignment data suggest for each of the *Paramecium* PKG isoforms a closer relationship to the Apicomplexan group than to the well-characterized type I and type II PKGs from higher eukaryotes (48, 60). For the latter, identities are only ~20% (Table 2). This is in contrast to the domain structures of the gene products, which much more closely resemble those from higher eukaryotes. These include a regulatory domain of two tandem cyclic nucleotide-binding sites flanked by an amino-terminal region for intracellular localization and a catalytic domain with highly conserved regions for ATP binding and catalysis (Fig.

3). Their calculated molecular masses range from 77.1 kDa to 94.8 kDa (Table 1). This is due not only to a variable N-terminal domain but also to the number of putative cGMP-binding sites within the regulatory domains of individual PKG subfamilies (Fig. 3). The consequences of both must be elucidated in future work.

**Immunolocalization of PKGs.** In order to analyze the sub-cellular distribution of PKGs, we have chosen the region between F266 and Q445 of PKG1-1 (Fig. 1A) for heterologous expression in *E. coli* (after changing all deviating *Paramecium* glutamine codons to universal glutamine codons) and the subsequent production of polyclonal Abs (Fig. 1F). This region is rather conserved between some of the isoforms (Table 3), and therefore a certain degree of cross-reactivity can be expected. However, cross-reactivity is likely to decrease rapidly with decreasing peptide similarities, as observed with some other PKG isoforms. The Abs easily recognized the recombinant peptide used for immunization when tested by an enzyme-linked immunosorbent assay and Western blotting (data not shown). They were used in an affinity-purified form for several approaches, including Western blotting and LM and EM localization studies.

In Western blots under semireducing conditions, whole-cell

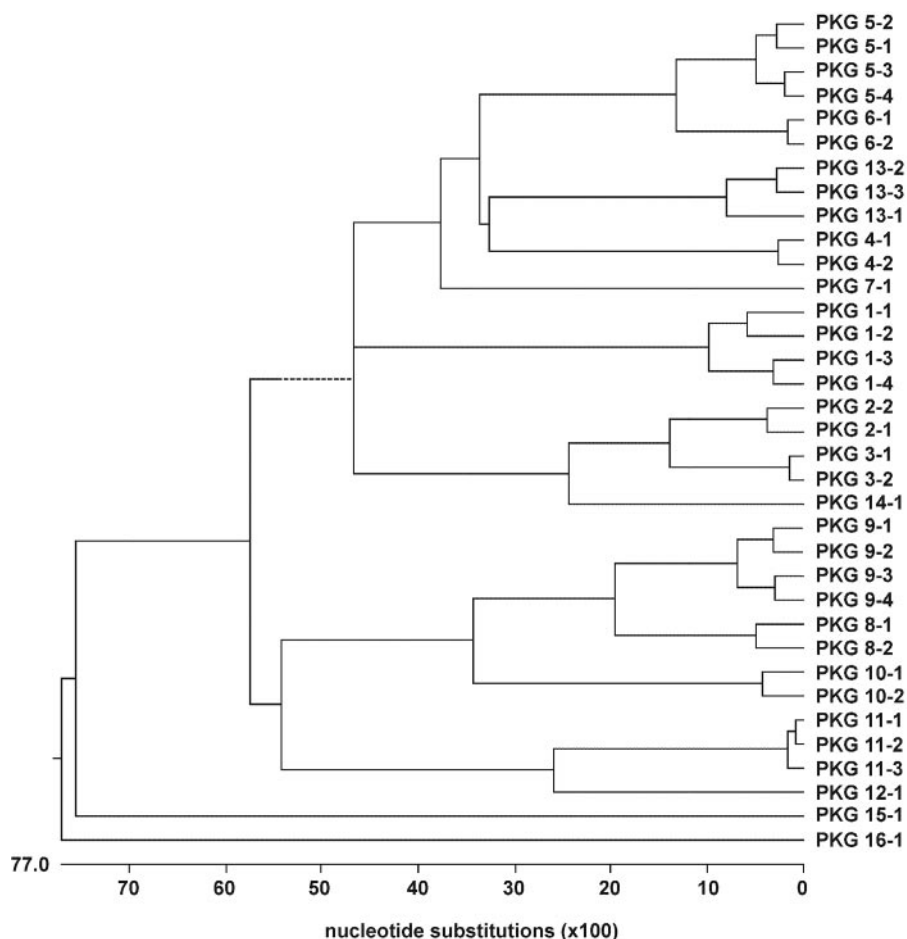


FIG. 2. Evolutionary relationships of the *Paramecium* PKG superfamily. Predictions from multiple sequence alignments are shown in a rooted phylogenetic tree generated with the Clustal W program of the DNASTAR Lasergene software (Madison, WI). The length of each pair of branches represents the distance between sequence pairs, while the units at the bottom of the tree indicate the numbers of substitution events. The scale below the tree indicates the numbers of “nucleotide substitutions” for both DNA and protein sequences. Note that most of the subfamilies contain two PKG genes (see the text).

homogenates displayed several cross-reactive bands with apparent molecular masses ranging between  $\sim 75$  and 150 kDa, which may represent not only monomeric but also homo- or heterodimeric forms of PKGs (Fig. 4). The latter is supported by the observation that some of the PKGs may contain putative leucine/isoleucine zipper motifs, which are, however, not highly conserved ( $<80\%$ ). Moreover, it cannot be entirely excluded that the polyclonal Ab may also recognize proteins other than PKG if they contain similar epitopes. However, this can be excluded, at least for a cAMP-dependent protein kinase of *Paramecium*, a closely related member of the same superfamily, as no cross-reactive bands of  $\sim 44$  kDa (10) were observed in the corresponding lanes (Fig. 4, lanes 6 to 10). Some of the bands occurred not only in the soluble fraction but also in particulate fractions, suggesting the existence of both soluble and membrane-associated isoforms. The same is true of the isolated cilium fraction, which preferentially contains PKG bands of  $\sim 150$  kDa, i.e., presumably dimeric forms, whereas a monomeric 83-kDa PKG species seems to be enriched selectively in the *Paramecium* cortex. None of the bands were visible when Western blots were produced with the corresponding

preimmune serum (Fig. 4, lanes 1 to 5) or in controls with the secondary Ab only (data not shown). Nevertheless, it cannot be entirely excluded that the polyclonal Ab may also recognize other proteins besides PKG when they also contain similar epitopes.

The occurrence of both soluble and structure-bound forms of PKGs within a *Paramecium* cell is also compatible with data obtained by confocal immunofluorescence analyses (Fig. 5). Besides some general cytosolic labeling, several subcellular organelles, such as cilia, the oral cavity, numerous vesicle-like structures, and some cortical structures, were distinctly labeled.

For most of the results achieved by confocal laser scanning microscopy (CLSM) analysis, we could identify equivalents in immunogold EM analyses (Fig. 6 and 7). Particularly consistent labeling occurred along the cell boundary formed by the intimately connected complex of the cell membrane and the outer part of the alveolar sac compartment, whose “inner” part (facing the cell center) was also labeled (Fig. 6A). Other “hot spots” in the cell cortex are the surroundings of trichocyst tips (Fig. 6A and B) and of ciliary basal bodies (Fig. 6A and 7A).

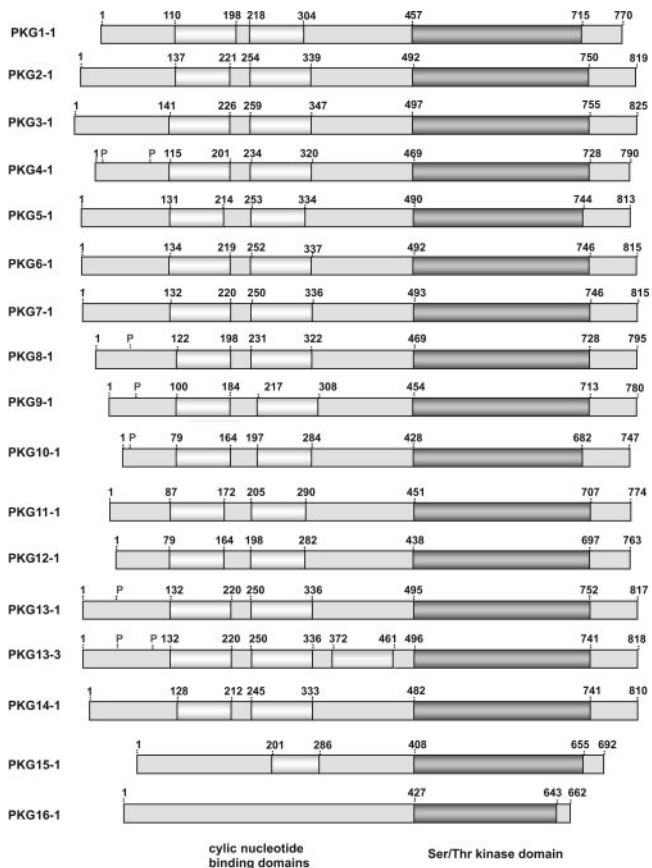


FIG. 3. Domain structures of individual members of the *Paramecium* PKG superfamily derived from conserved motif searching. Characteristic features are shown as follows: light gray, cyclic nucleotide-binding domains; dark gray, catalytic domain; and P, potential autophosphorylation sites. Note the variance in the number of cyclic GMP-binding domains within individual PKG subfamilies.

The most consistently labeled structures were the membranes of cilia (Fig. 6C and D). Less densely labeled areas were the surface membranes and basal bodies along the oral cavity (Fig. 7B) and cytoplasmic domains around vesicles presumably involved in trafficking. In the cortex, this includes regions with medium-sized vesicles and the endoplasmic reticulum (Fig. 7A). Deeper in the cytoplasm, domains with “discoidal vesicles” (engaged in recycling from the phagocytic vacuoles and the cytoproct to the oral cavity [1]) and the surfaces of larger vesicles attributable to the phagolysosomal apparatus (Fig. 7C) were labeled.

In total, the results obtained by immuno-EM analysis are fully compatible with those from immunofluorescence analysis (Fig. 5), including labeling of the oral cavity, cilia, vesicle-type structures, and elements of the cell cortex.

**pp63/pf as putative substrate for PKG.** Since PKGs seem to be enriched in cortical structures, we were interested in whether pp63/pf, an exocytosis-sensitive phosphoprotein of 63 kDa which is rapidly (within 0.1 s) dephosphorylated upon stimulation and slowly rephosphorylated during  $\leq 1$  min (31, 87), would be a putative candidate for an endogenous substrate, inasmuch as it is also a soluble protein that occurs in the cortex (38). In order to establish pp63/pf as a putative PKG

TABLE 3. Comparison of PKG regions used for raising polyclonal Abs

Protein	Region (aa)	Length (aa)	Identity <sup>a</sup> (%)
PKG1-1	F266–Q445	180	100
PKG1-2	F266–R445	180	89.4
PKG1-3	F266–Q445	180	85.6
PKG1-4	F266–Q445	180	85.6
PKG2-1	F302–R481	180	38.3
PKG2-2	F302–R481	180	38.9
PKG3-1	F307–R486	180	34.4
PKG3-2	F307–R486	180	34.4
PKG4-1	F282–Y457	176	42.2
PKG4-2	F282–Q457	176	41.7
PKG5-1	L296–Q474	179	41.1
PKG5-2	L296–Q474	179	41.1
PKG5-3	L290–Q468	179	41.7
PKG5-4	L290–Q468	179	41.7
PKG6-1	L300–Q476	177	41.1
PKG6-2	L300–Q476	177	42.8
PKG7-1	F298–S478	181	41.7
PKG8-1	F280–Q456	177	22.2
PKG8-2	F280–Q456	177	20.6
PKG9-1	F266–A441	176	24.4
PKG9-2	F266–A441	176	23.9
PKG9-3	F264–A439	176	23.3
PKG9-4	F264–A439	176	22.8
PKG10-1	F246–N412	167	23.3
PKG10-2	F246–N412	167	25.0
PKG11-1	F253–T435	183	35.6
PKG11-2	F253–T435	183	35.6
PKG11-3	F254–T436	183	35.6
PKG12-1	F245–T425	181	32.8
PKG13-1	F298–A481	184	36.1
PKG13-1	F298–V481	184	36.1
PKG13-3	F298–V481	184	36.7
PKG14-1	F298–V481	179	33.3
PKG15-1	F248–R396	149	22.2
PKG16-1	Y238–K388	151	16.7

<sup>a</sup> *Paramecium* PKG protein sequences of the corresponding regions were aligned using the Clustal W program.

substrate, we used a chromatographically enriched PKG fraction for in vitro phosphorylation studies with recombinant pp63/pf. As shown in Fig. 8, recombinant pp63/pf was intensely phosphorylated under conditions when PKGs were fully stimulated (lanes 5 and 6). Under conditions of autophosphorylation (without recombinant pp63/pf), we were also able to identify several phosphorylation bands between 75 and 105 kDa (Fig. 8, lane 3). Similar bands have also been observed in Western blots and therefore may represent autophosphorylated forms of PKGs rather than copurified substrate proteins. The specificity of these phosphorylation studies is also supported by the finding that enzyme activity is stimulated by cGMP (compare Fig. 8, lane 2, with lanes 5 and 6) but not by cAMP (data not shown).

## DISCUSSION

**General aspects.** Unlike higher eukaryotic cells, *Paramecium* is not known to perform alternative splicing of mRNAs. Diversification of PKGs may therefore be achieved by increasing gene numbers, probably facilitated by recent whole-genome duplication (L. Sperling and J. Cohen, personal communication). In mammals, splice variants of PKG occur (19, 48)

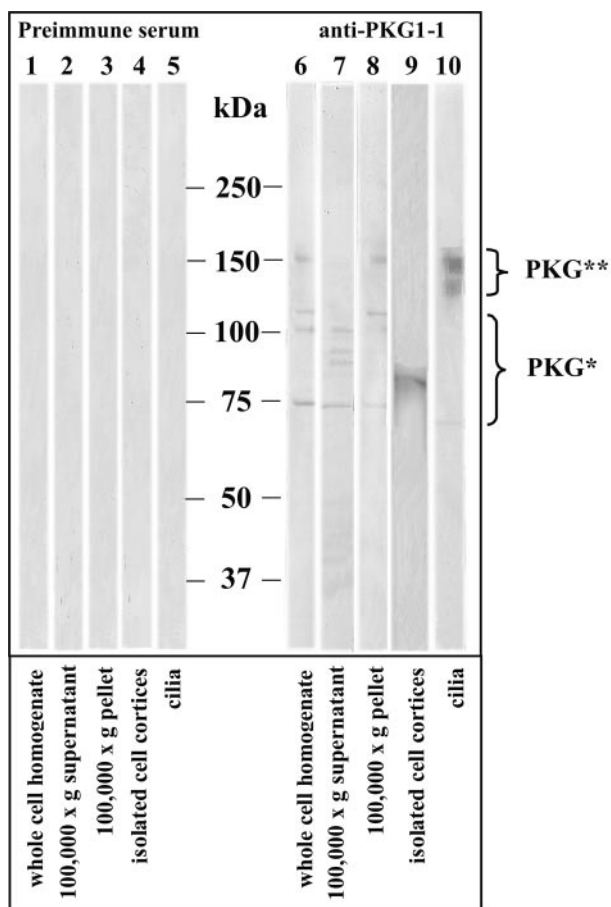


FIG. 4. Western blot analysis of the subcellular distribution of PKGs, using Abs against a cross-reactive region of PKG1-1. Aliquots (50  $\mu$ g) of whole-cell homogenates (lanes 1 and 6), supernatants from centrifugation at 100,000  $\times$  g (lanes 2 and 7), pellets from centrifugation at 100,000  $\times$  g (lanes 3 and 8), isolated cell cortices (lanes 4 and 9), and isolated cilia (lanes 5 and 10) were processed for immunobinding using either polyclonal affinity-purified Abs against the recombinant PKG1-1 peptide shown in Fig. 1E (lanes 6 to 10) or the corresponding preimmune serum (lanes 1 to 5). Several cross-reactive bands between  $\sim$ 70 kDa and 150 kDa were observed, not only in the 100,000  $\times$  g supernatant fraction (lane 7) but also in particulate fractions (lanes 8 and 9), suggesting the existence of both soluble and membrane-associated isoforms as well as of monomeric (\*) and homo- or heterodimeric (\*\*) forms of PKGs. The same was true for isolated cilia (lane 10), although cilia may preferentially contain dimeric forms of PKGs, an interesting aspect to be analyzed in future work. This is in contrast to the cortex fraction (lane 9), which was devoid of cilia and contained a strong band of 83 kDa. None of the bands were detected by the corresponding preimmune serum (lanes 1 to 5).

which are either differentially located, just like PKG isoforms in *Drosophila* Malpighian tubule cells (50), or regulate the expression of another isoform (21). One may speculate that some of the paralogs we found in *Paramecium* may potentially exert such a regulatory function. Moreover, the plethora of PKG gene products may contribute to the regulation of the elaborated vesicle trafficking system and to the elaborated surface patterning of a *Paramecium* cell with their clear-cut functional domains.

**Gene structure and domains of PKG molecules.** The gene structures of the PKG 1 and PKG 2 subfamilies, shown in Fig.

1, fulfill a variety of criteria typical of PKGs, e.g., of mammalian species (19, 48). (i) They represent single molecules with typical molecular masses, thus fitting with PKG fractions isolated from *Paramecium* cells (53) or from other lower eukaryotic cells (55, 80), including Apicomplexan parasites (16, 23). This is in contrast to cAMP-dependent protein kinases, including those from *Paramecium* (9; R. Kissmehl and H. Plattner, unpublished observation), which possess separate catalytic and regulatory subunits. (ii) Most of the *Paramecium* PKGs possess a molecular organization characteristic of mammalian PKGs (19, 48), including a regulatory part with two cGMP-binding domains in the N-terminal half and a catalytic (kinase) domain in the C-terminal half, with considerable similarities in the deduced amino acid sequences (Table 2). (iii) They display most of the relevant motifs typical of PKGs (19, 48), with the exception that the amino-terminal domains of PKG1-1 and PKG2-1 seem to have neither a dimerization site (no conserved leucine/isoleucine heptad repeat) nor an autoinhibitory region. The latter is also true for the other PKG paralogs in *Paramecium* compared with the consensus sequence K/R-K/R-X-G/A-S-E-P/S described previously (60).

An interesting aspect also comprises the variable numbers of putative cGMP-binding domains within the regulatory domains of individual PKG subfamilies (Fig. 3). Although their individual properties still have to be elucidated in future work, e.g., binding affinities, dissociation kinetics, etc., the relevance and consequences of this heterogeneity, together with the large number of PKG paralogs, may reflect the responsiveness of *Paramecium* cells to widely varying environmental conditions. It would also be interesting to know whether and how PKG paralogs with nonconserved cGMP-binding domains, such as PKG16-1, may be able to contribute as effectors for cGMP.

**Comparison with other Alveolata.** Parasitic relatives, such as *Plasmodium falciparum*, have larger PKG molecules deduced from larger genes, with three active and a degenerate fourth cGMP-binding domain (11, 12). PKGs from *Eimeria tenella* have three cGMP-binding domains, and two isoforms are formed from a single-copy gene by alternative translation initiation (23). Interestingly, the overall domain structure of most of the PKG genes of *Paramecium* therefore resembles much more those from less related species, such as mammals or plants, than those from their closest parasitic relatives. However, the similarity is much closer when the domains of PKGs are compared at the amino acid level (Table 2).

**Localization and potential functions of PKGs.** For *Paramecium*, no data are available on cGMP-sensitive ion channels or cGMP-activated PD activity, while the occurrence of PKG activity is well established (53). Previous attempts to localize PKGs in *Paramecium* (41) are difficult to interpret, in contrast to the case of GC. The latter has been clearly localized to ciliary membranes, to the complex formed by the outer alveolar sac membrane and the cell membrane, and to the lower (inner) part of the alveolar sac envelope (47). In conceivable agreement with this is the immunofluorescence localization of PKG in cilia and some cell surface compartments (Fig. 6), which in part is reminiscent of green fluorescent protein-labeled alveolar sacs (27). This would suggest a rapid and well-localized interaction between cGMP, after formation by GC, and PKG. The question becomes, then, what may be the functional implications of this interaction?

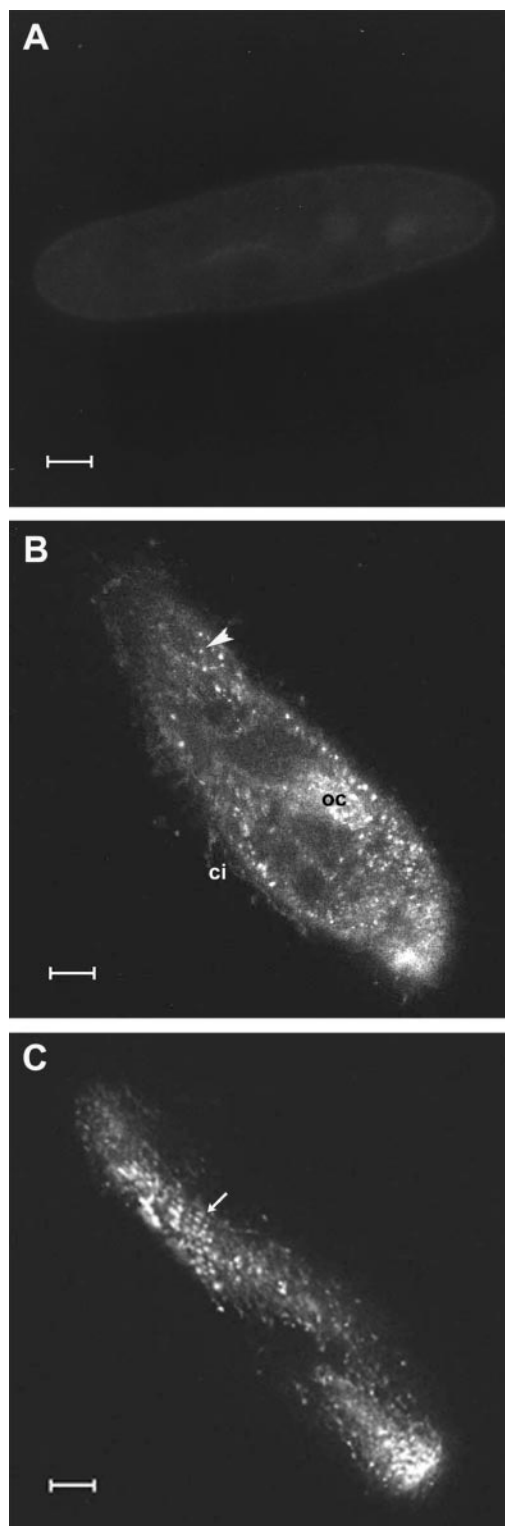


FIG. 5. Immunofluorescence localization of PKGs by CLSM. Cells permeabilized under conditions preserving cilia were labeled either by affinity-purified Abs against a cross-reactive region of PKG1-1 (B and C) or with the corresponding preimmune serum (A). Besides slight cytosolic labeling, several subcellular organelles were much more intensely labeled, including cilia (ci), the oral cavity (oc), numerous vesicle-like structures (arrowhead, B), and various structures occurring at the cell cortex (arrow, C). No signal was observed with the preimmune serum (A). Bars = 10  $\mu\text{m}$ .

**Relevance of PKGs for ciliary activity.** Ciliary beat activity in *Paramecium* is rapidly reversed by depolarization-dependent  $\text{Ca}^{2+}$  influx (17), and this process seems to be modulated by a [cGMP] increase (51, 59). cGMP, in turn, is produced by  $\text{Ca}^{2+}$ -dependent GC activation. Concomitantly,  $\text{Ca}^{2+}$  has been established as the primary signal, since pressure injection of cGMP under voltage clamp conditions does not change the ciliary beat direction (56). Furthermore, when cGMP is applied in vitro to permeabilized *Paramecium* models, it increases the beat frequency without changing its direction, with only a minor change in the beating pattern (8). Surprisingly, the overall reaction is not much different from the effects of cAMP. An increase in cAMP, as it occurs upon hyperpolarization, is accompanied by an increased ciliary beat frequency without any change in swimming direction (84). Thus, the [cGMP] increase seen during depolarization is at odds with the absence of a reversal effect of cGMP application in vitro. How can this be reconciled?

One reason could be the lack of signal transduction in the absence of PKGs, assuming extraction during cell permeabilization. In fact, at least some of the PKGs are soluble (see Results), e.g., the enzyme extracted from cilia under previously described conditions (53). If so, the involvement of PKGs would be plausible despite the restricted effects of cGMP in vitro. Concomitantly, the application of PKGs to permeabilized *Paramecium* cells induces ciliary reversal in *atalanta A* mutants, which normally do not show this reaction (3). Although a ciliary protein of 59 kDa can be selectively phosphorylated in vitro in a cGMP-dependent manner (3), less is known about PKGs and the molecular machinery regulating ciliary beat direction in *Paramecium*. However, the involvement of PKGs appears to be very likely due to the three forms that have been extracted in previous biochemical work (53).

**Potential relevance for exo-endocytosis.** In metazoan cells, the global response generally achieved by PKG activation is lowering the intracellular [ $\text{Ca}^{2+}$ ] and therefore reestablishing [ $\text{Ca}^{2+}$ ] homeostasis (30, 48, 77). This may also hold for *Paramecium* because of the following observations. (i) GC is associated with alveolar sac membranes (47), which are established cortical  $\text{Ca}^{2+}$  stores activated upon exocytosis stimulation (61). (ii) [cGMP] rises during exocytosis stimulation (42), although this lags behind the  $\text{Ca}^{2+}$  signal determined by fast fluorochrome analyses or by analytical EM methods, i.e., quenched-flow/X-ray microanalysis (= "EDX") (61). Both of these methods provide considerable spatial resolution, while the [cGMP] changes could be measured, although quickly, only globally. (iii) During exocytosis, a 63-kDa phosphoprotein, pp63/pf, is rapidly dephosphorylated within 0.1 s and slowly rephosphorylated during  $\leq 1$  min (31, 75, 87). It is localized in the cell cortex (38), as is PKG (this paper). The gene has been cloned, and the recombinant expression product showed phosphoglucosyltransferase activity (26). The actual Ser/Thr phosphorylation sites have been determined by matrix-assisted laser desorption ionization analysis and prognosticated as sites for casein kinase 2 and PKG activities (43). Based on structure analysis by X-ray diffraction, phosphorylation sites could be positioned on the surface of the pp63/pf molecule so that they are accessible to the respective kinases (54). The predicted phosphorylation of pp63/pf has been verified previously for casein kinase 2 (37, 79). In the present paper, we have achieved this for PKGs,

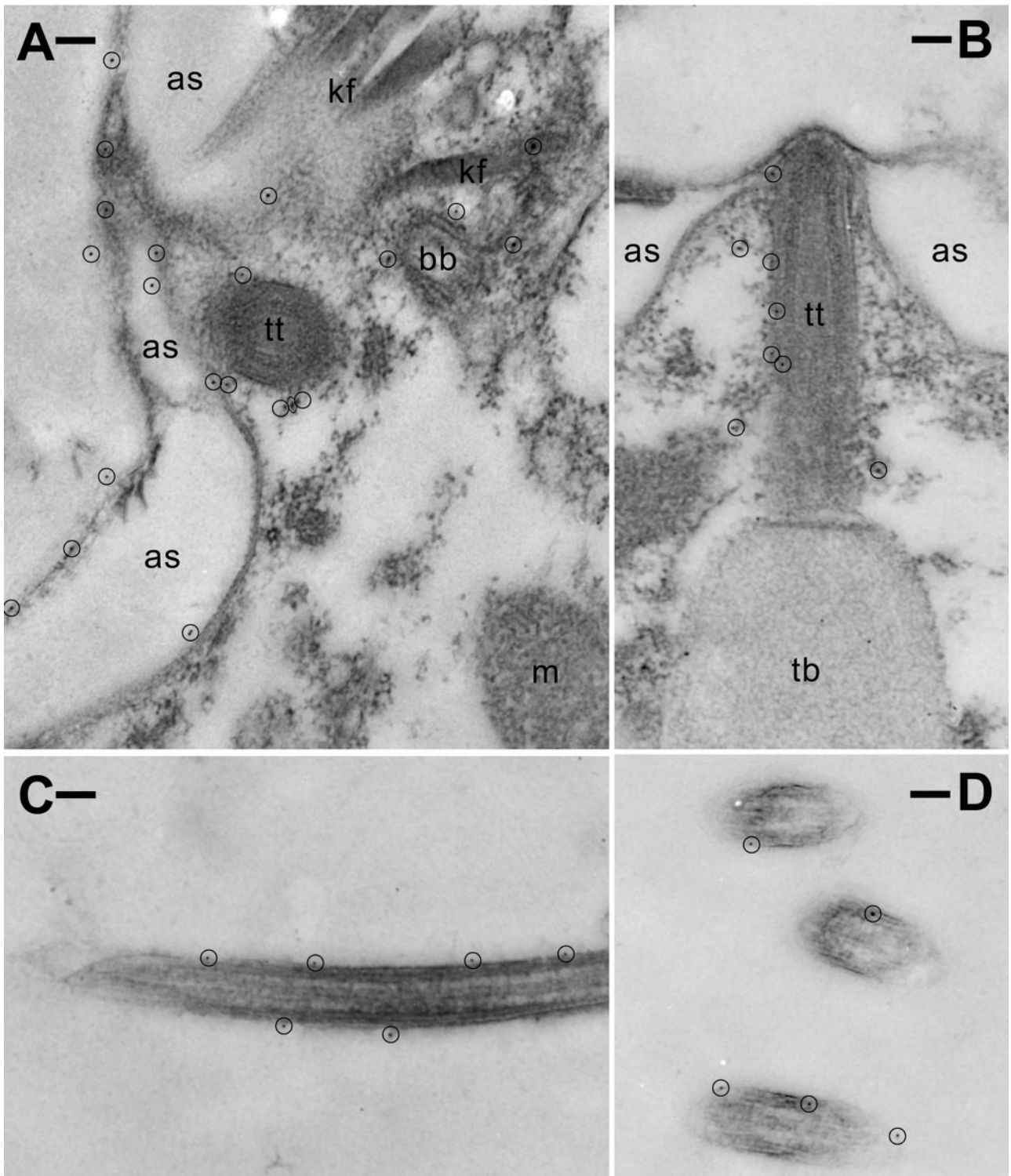


FIG. 6. Immunogold EM localization of PKGs. (A) The structures most heavily labeled with  $Au_{5\text{ nm}}$  particles (encircled) are complexes formed by the cell membrane and the tightly apposed outer part of the alveolar sac (as) membrane (left side). Additional labeling occurs on the inner part of the alveolar sac membrane, around a trichocyst tip (tt), and around a ciliary basal body (bb). Note the absence of the label from "irrelevant" structures, such as the outside medium, lumens of alveolar sacs, kinodesmal fibers (kf), and a mitochondrion (m). (B) Enrichment of  $Au_{5\text{ nm}}$  along the flanks of a trichocyst tip, in contrast to the trichocyst body (tb), shown below. (C and D) Labeling was predominantly enriched along the membranes of cilia, as shown in longitudinal (C) and cross (D) sections. Bars = 0.1  $\mu\text{m}$ .

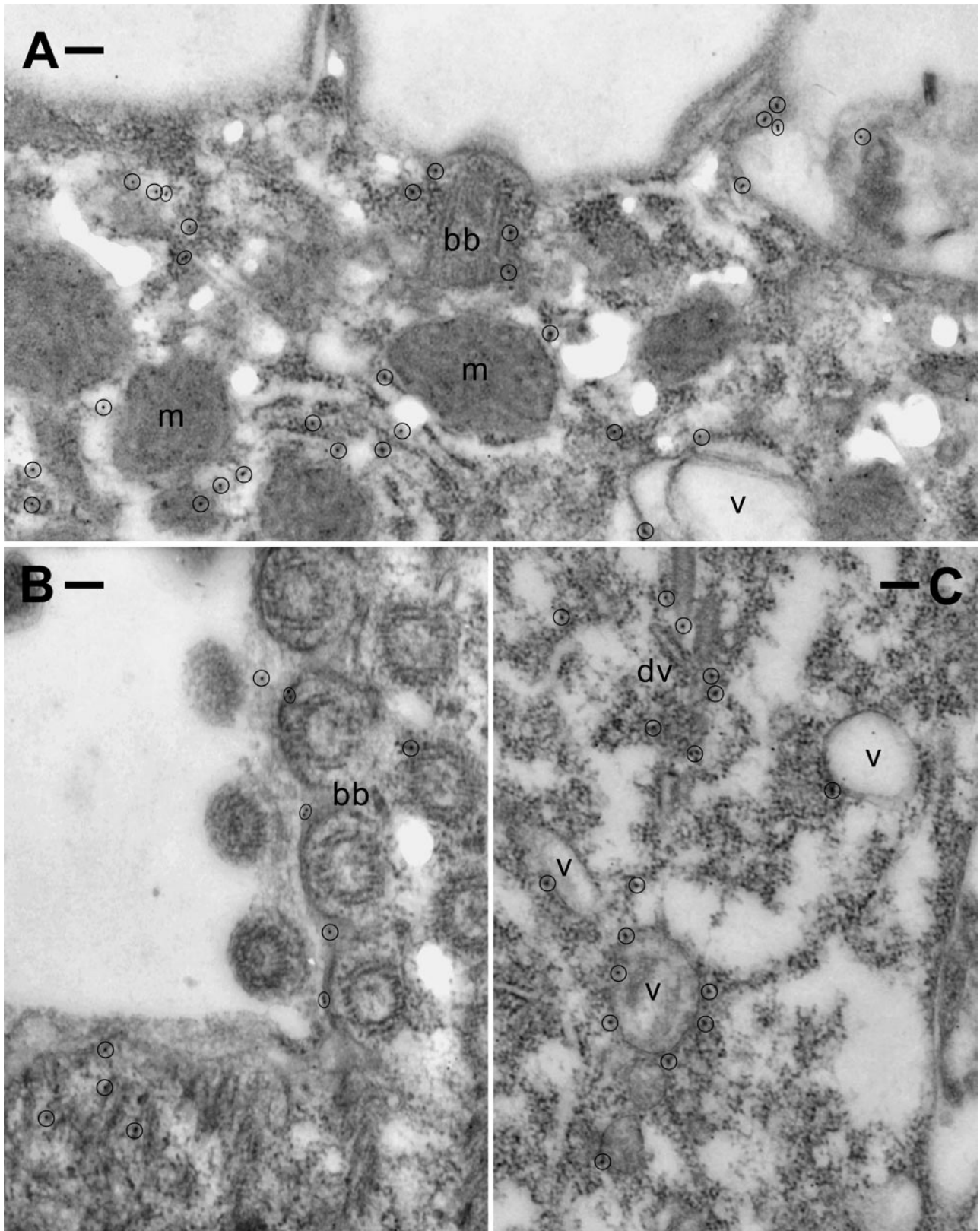


FIG. 7. Immunogold EM localization. (A) Cortical labeling ( $Au_{5\text{ nm}}$  [encircled]) of "hot spots" on the cell surface (cell membrane-alveolar sac complex, top right), around a ciliary basal body (bb), and in association with the endoplasmic reticulum and vesicles (v) of different sizes. (B) Oral cavity with label on the cell membrane near basal bodies (bb). (C) Labeling of discoidal vesicles (dv) and of larger, round to oblong vesicles (v), probably members of the lysosomal apparatus. Bars = 0.1  $\mu\text{m}$ .

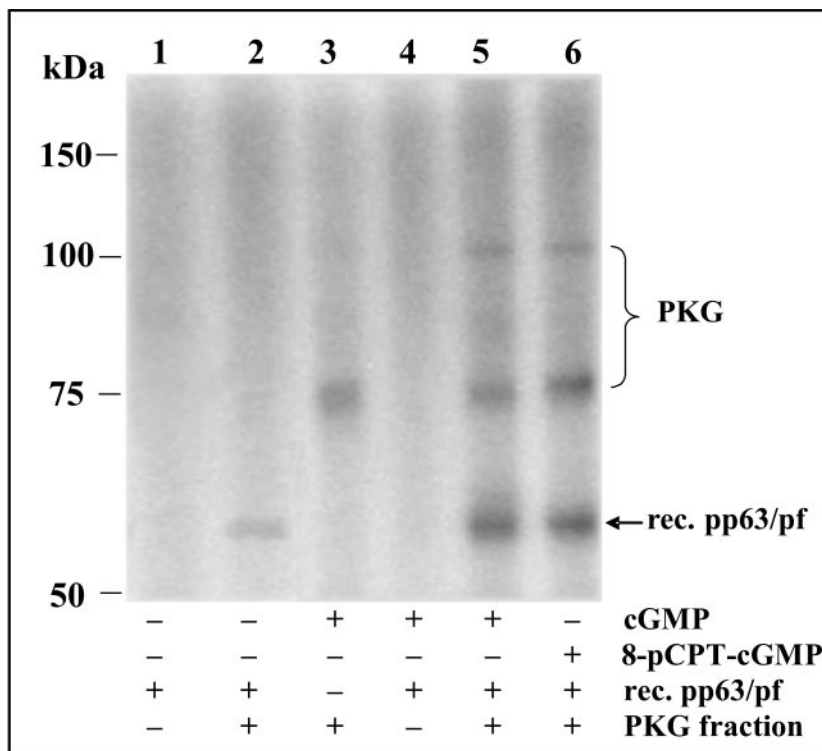


FIG. 8. Phosphorylation of recombinant pp63/pf by endogenous PKG in vitro. Phosphorylation of recombinant pp63/pf was observed when 3  $\mu$ g of recombinant pp63/pf (lanes 1, 2, 4, 5, and 6) was assayed with  $\sim 1.25$   $\mu$ g of a PKG-containing fraction (lanes 2, 3, 5, and 6) either in the absence (lane 2) or in the presence of 0.15  $\mu$ M cGMP (lane 5) or 0.15  $\mu$ M 8-pCPT-cGMP (lane 6). The other two bands, at  $\sim 75$  and 100 kDa, were also observed under autophosphorylation conditions in the PKG fraction (without pp63/pf, lane 3). Note the stimulatory effect of cGMP on the phosphorylation of pp63/pf (compare lane 2 with lanes 5 and 6). In contrast, recombinant pp63-1/pf was not phosphorylated when assayed under similar conditions in the absence of PKG (lanes 1 and 4).

although the precise PKG form(s) contributing remains to be identified. A putative role of this phosphorylation has already been discussed recently (63), including regulating contact with substrate proteins (7).

In summary, considering exo-endocytosis-regulated processes, the potential role of PKG involvement is not less intriguing than, for instance, the level of discussion concerning neuronal (14, 85) and a variety of other systems (20, 22).

**Relevance for other activities in *Paramecium*.** Other  $\text{Ca}^{2+}$ -based signaling mechanisms in *Paramecium* include spontaneous circadian rhythms involving  $\text{Ca}^{2+}$  and cGMP/cAMP oscillations (25), unfortunately with unknown signal transduction pathways. In this regard, periodic cGMP changes and the involvement of PKGs have been established for some mammalian neurons (74).

PKG-mediated phosphorylation processes have recently been extended to Rac-type proteins (32), with an involvement of cytoskeleton structuring and vesicle trafficking. The latter is highly diversified in *Paramecium*, where it awaits an in-depth molecular analysis (62).

**Conclusions.** We could establish in *P. tetraurelia* cells the occurrence of an unexpectedly large family of PKG genes. The large number is not surprising if one considers the large number of sequences altogether coding for protein kinases, as found already at an early stage of the *Paramecium* genome project (72). The different PKG isoforms may serve specific

functions depending on their positions in the cell. In cilia, PKGs can phosphorylate proteins to be more clearly defined. Their potential role as a switch for changing ciliary beat direction has yet to be established in detail. In the cell soma of *Paramecium*, PKGs will perform independent activities, e.g., in the context of rephosphorylation of the exocytosis-sensitive phosphoprotein pp63/pf. The data presented here will allow one to address these questions in much more detail beyond the biochemical data previously published.

#### ACKNOWLEDGMENTS

We gratefully thank Jean Cohen for access to the library screening, J. E. Schultz (University of Tübingen) for providing us with the genomic *Paramecium* library, Claudia Stuermer for access to the CLSM, Ivonne Sehring for excellent technical help in the CLSM analysis, and Doris Bliestle for electronic image processing.

This work was supported by Deutsche Forschungsgemeinschaft grants to H.P.

#### REFERENCES

- Allen, R. D., and A. K. Fok. 2000. Membrane trafficking and processing in *Paramecium*. *Int. Rev. Cytol.* **198**:277–317.
- Altschul, S. F., T. L. Madden, A. A. Schaffer, J. Zhang, Z. Zhang, W. Miller, and D. J. Lipman. 1997. Gapped BLAST and PSI-BLAST: a new generation of protein database search programs. *Nucleic Acids Res.* **25**:3389–3402.
- Ann, K. S., and D. L. Nelson. 1995. Protein substrates for cGMP-dependent protein phosphorylation in cilia of wild type and *atalanta* mutants of *Paramecium*. *Cell Motil. Cytoskel.* **30**:252–260.
- Antal, Z., C. Rasclé, M. Fevre, and C. Bruel. 2004. Single oligonucleotide

- nested PCR: a rapid method for the isolation of genes and their flanking regions from expressed sequence tags. *Curr. Genet.* **46**:240–246.
5. Atkinson, R. A., V. Saudek, J. P. Huggins, and J. T. Pelton. 1991. 1H NMR and circular dichroism studies of the N-terminal domain of cyclic GMP dependent protein kinase: a leucine/isoleucine zipper. *Biochemistry* **30**:9387–9395.
  6. Bairoch, A., P. Bucher, and K. Hofmann. 1997. The PROSITE database, its status in 1997. *Nucleic Acids Res.* **25**:217–221.
  7. Barinaga, M. 1999. New clues to how proteins link up to run the cell. *Science* **283**:1247–1249.
  8. Bonini, N. M., and D. L. Nelson. 1988. Differential regulation of *Paramecium* ciliary motility by cAMP and cGMP. *J. Cell Biol.* **106**:1615–1623.
  9. Carlson, G. L., and D. L. Nelson. 1995. Isolation and characterization of protein kinases from *Paramecium* cilia. *Methods Cell Biol.* **47**:473–480.
  10. Carlson, G. L., and D. L. Nelson. 1996. The 44-kDa regulatory subunit of the *Paramecium* cAMP-dependent protein kinase lacks a dimerization domain and may have a unique autophosphorylation site sequence. *J. Eukaryot. Microbiol.* **43**:347–356.
  11. Deng, W., and D. A. Baker. 2002. A novel cyclic GMP-dependent protein kinase is expressed in the ring stage of the *Plasmodium falciparum* life cycle. *Mol. Microbiol.* **44**:1141–1151.
  12. Deng, W., A. Parbhu-Patel, D. J. Meyer, and D. A. Baker. 2003. The role of two novel regulatory sites in the activation of the cGMP-dependent protein kinase from *Plasmodium falciparum*. *Biochem. J.* **374**:559–565.
  13. Dessen, P., M. Zagulski, R. Gromadka, H. Plattner, R. Kissmehl, E. Meyer, M. Bétermier, J. E. Schultz, J. U. Linder, R. E. Pearlman, C. Kung, J. Forney, B. H. Satir, J. Van Houten, A. M. Keller, M. Froissard, L. Sperling, and J. Cohen. 2001. *Paramecium* genome survey: a pilot project. *Trends Genet.* **17**:306–308.
  14. DeVente, J., E. Asan, S. Gambaryan, M. Markerink-van Ittersum, H. Axer, K. Gallatz, S. M. Lohmann, and M. Palkovits. 2001. Localization of cGMP-dependent protein kinase type II in rat brain. *Neuroscience* **108**:27–49.
  15. Dillon, P. J., and C. A. Rosen. 1993. Use of polymerase chain reaction for the rapid construction of synthetic genes. *Methods Mol. Biol.* **15**:263–269.
  16. Donald, R. G. K., J. Allocco, S. B. Singh, B. Nare, S. P. Salowe, J. Wiltsie, and P. A. Liberator. 2002. *Toxoplasma gondii* cyclic GMP-dependent kinase: chemotherapeutic targeting of an essential parasite protein kinase. *Eukaryot. Cell* **1**:317–328.
  17. Eckert, R., and P. Brehm. 1979. Ionic mechanisms of excitation in *Paramecium*. *Annu. Rev. Biophys. Bioeng.* **8**:353–383.
  18. Feil, R., J. Kellermann, and F. Hofmann. 1995. Functional cGMP-dependent protein kinase is phosphorylated in its catalytic domain at threonine-516. *Biochemistry* **34**:13152–13158.
  19. Francis, S. H., and J. D. Corbin. 1994. Structure and function of cyclic nucleotide-dependent protein kinases. *Annu. Rev. Physiol.* **56**:237–272.
  20. Gambaryan, S., C. Wagner, A. Smolenski, U. Walter, W. Poller, W. Haase, A. Kurtz, and S. M. Lohmann. 1998. Endogenous or overexpressed cGMP-dependent protein kinases inhibit cAMP-dependent renin release from rat isolated perfused kidney, microdissected glomeruli, and isolated juxtaglomerular cells. *Proc. Natl. Acad. Sci. USA* **95**:9003–9008.
  21. Gambaryan, S., A. Palmethofer, M. Glazova, A. Smolenski, G. I. Kristjansson, M. Zimmer, and S. M. Lohmann. 2002. Inhibition of cGMP-dependent protein kinase II by its own splice isoform. *Biochem. Biophys. Res. Commun.* **293**:1438–1444.
  22. Gambaryan, S., E. Butt, K. Marcus, M. Glazova, A. Palmethofer, G. Guillon, and A. Smolenski. 2003. cGMP-dependent protein kinase type II regulates basal level of aldosterone production by zona glomerulosa cells without increasing expression of the steroidogenic acute regulatory protein gene. *J. Biol. Chem.* **278**:29640–29648.
  23. Gurnett, A. M., P. A. Liberator, P. M. Dulski, S. P. Salowe, R. G. K. Donald, J. W. Anderson, J. Wiltsie, C. A. Diaz, G. Harris, B. Chang, S. J. Darkin-Ratray, B. Nare, T. Crumley, P. S. Blum, A. S. Misura, T. Tamas, M. K. Sardana, J. Yuan, T. Biftu, and D. M. Schmatz. 2002. Purification and molecular characterization of cGMP-dependent protein kinase from *Apicomplexan* parasites. A novel chemotherapeutic target. *J. Biol. Chem.* **277**:15913–15922.
  24. Hanks, S. K., and T. Hunter. 1995. The eukaryotic protein kinase superfamily: kinase (catalytic) domain structure and classification. *FASEB J.* **9**:576–596.
  25. Hasegawa, K., H. Kikuchi, S. Ishizaki, A. Tamura, Y. Tsukahara, Y. Nakaoka, E. Iwai, and T. Sato. 1999. Simple fluctuation of Ca<sup>2+</sup> elicits the complex circadian dynamics of cyclic AMP and cyclic GMP in *Paramecium*. *J. Cell Sci.* **112**:201–207.
  26. Hauser, K., R. Kissmehl, J. Linder, J. E. Schultz, F. Lottspeich, and H. Plattner. 1997. Identification of isoforms of the exocytosis-sensitive phosphoprotein pp63/parafusin in *Paramecium tetraurelia* and demonstration of phosphoglucomutase activity. *Biochem. J.* **323**:289–296.
  27. Hauser, K., N. Pavlovic, N. Klauke, D. Geissinger, and H. Plattner. 2000. Green fluorescent protein-tagged sarco(endo)plasmic reticulum Ca<sup>2+</sup>-ATPase overexpression in *Paramecium* cells: isoforms, subcellular localization, biogenesis of cortical calcium stores and functional aspects. *Mol. Microbiol.* **37**:773–787.
  28. Haynes, W. J., K. Y. Ling, Y. Saimi, and C. Kung. 1995. Induction of antibiotic resistance in *Paramecium tetraurelia* by the bacterial gene APH-3'-II. *J. Eukaryot. Microbiol.* **42**:83–91.
  29. Haynes, W. J., B. Vaillant, R. R. Preston, Y. Saimi, and C. Kung. 1998. The cloning by complementation of the pawn-A gene in *Paramecium*. *Genetics* **149**:947–957.
  30. Hofmann, F. 2005. The biology of cyclic GMP-dependent protein kinases. *J. Biol. Chem.* **280**:1–4.
  31. Höhne-Zell, B., G. Knoll, U. Riedel-Gras, W. Hofer, and H. Plattner. 1992. A cortical phosphoprotein ("pp63") sensitive to exocytosis triggering in *Paramecium* cells. Immuno-localization and quenched-flow correlation of time course of dephosphorylation with membrane fusion. *Biochem. J.* **286**:843–849.
  32. Hou, Y., R. D. Ye, and D. D. Browning. 2004. Activation of the small GTPase Rac1 by cGMP-dependent protein kinase. *Cell Signal.* **16**:1061–1069.
  33. Jarchau, T., C. Hausler, T. Markert, D. Pöhler, J. VanDekerckhove, H. R. DeJonge, S. M. Lohmann, and U. Walter. 1994. Cloning, expression, and in situ localization of rat intestinal cGMP-dependent protein kinase II. *Proc. Natl. Acad. Sci. USA* **91**:9426–9430.
  34. Keller, A. M., and J. Cohen. 2000. An indexed genomic library for *Paramecium* complementation cloning. *J. Eukaryot. Microbiol.* **47**:1–6.
  35. Kemp, B. E., and R. B. Pearson. 1991. Intracellular regulation of protein kinases and phosphatases. *Biochim. Biophys. Acta* **1094**:67–76.
  36. Kissmehl, R., T. Treptau, H. W. Hofer, and H. Plattner. 1996. Protein phosphatase and kinase activities possibly involved in exocytosis regulation in *Paramecium tetraurelia*. *Biochem. J.* **317**:65–76.
  37. Kissmehl, R., T. Treptau, K. Hauser, and H. Plattner. 1997. A novel, calcium-inhibitable casein kinase in *Paramecium* cells. *FEBS Lett.* **402**:227–235.
  38. Kissmehl, R., K. Hauser, M. Gössringer, M. Momayez, N. Klauke, and H. Plattner. 1998. Immunolocalization of the exocytosis-sensitive phosphoprotein, pp63/parafusin, in *Paramecium* cells using antibodies against recombinant protein. *Histochem. Cell Biol.* **110**:1–8.
  39. Kissmehl, R., M. Froissard, H. Plattner, M. Momayez, and J. Cohen. 2002. NSF regulates membrane traffic along multiple pathways in *Paramecium*. *J. Cell Sci.* **115**:3935–3946.
  40. Kissmehl, R., I. M. Sehring, E. Wagner, and H. Plattner. 2004. Immunolocalization of actin in *Paramecium* cells. *J. Histochem. Cytochem.* **52**:1543–1559.
  41. Klumpp, S., A. L. Steiner, and J. E. Schultz. 1983. Immunocytochemical localization of cyclic GMP, cGMP-dependent protein kinase, calmodulin and calcineurin in *Paramecium tetraurelia*. *Eur. J. Cell Biol.* **32**:164–170.
  42. Knoll, G., D. Kerboef, and H. Plattner. 1992. A rapid calcium influx during exocytosis in *Paramecium* cells is followed by a rise in cyclic GMP within 1 s. *FEBS Lett.* **304**:265–268.
  43. Kussmann, M., K. Hauser, R. Kissmehl, J. Breed, H. Plattner, and P. Roepstorff. 1999. Comparison of in vivo and in vitro phosphorylation of the exocytosis-sensitive protein pp63/parafusin by differential MALDI mass spectrometric peptide mapping. *Biochemistry* **38**:7780–7790.
  44. Kyte, J., and R. F. Doolittle. 1982. A simple method for displaying the hydrophobic character of a protein. *J. Mol. Biol.* **157**:105–132.
  45. Landgraf, W., R. Hullin, C. Göbel, and F. Hofmann. 1986. Phosphorylation of cGMP-dependent protein kinase increases the affinity for cyclic AMP. *Eur. J. Biochem.* **154**:113–117.
  46. Landgraf, W., and F. Hofmann. 1989. The amino terminus regulates binding to and activation of cGMP-dependent protein kinase. *Eur. J. Biochem.* **181**:643–650.
  47. Linder, J. U., P. Engel, A. Reimer, T. Krüger, H. Plattner, A. Schultz, and J. E. Schultz. 1999. Guanylyl cyclases with the topology of mammalian adenylyl cyclases and an N-terminal P-type ATPase-like domain in *Paramecium*, *Tetrahymena* and *Plasmodium*. *EMBO J.* **18**:4222–4232.
  48. Lohmann, S. M., A. B. Vaandrager, A. Smolenski, U. Walter, and H. R. DeJonge. 1997. Distinct and specific functions of cGMP-dependent protein kinases. *Trends Biochem. Sci.* **22**:307–312.
  49. Lumpert, C. J., H. Kerken, and H. Plattner. 1990. Cell surface complexes ("cortices") isolated from *Paramecium tetraurelia* cells as a model system for analysing exocytosis *in vitro* in conjunction with microinjection studies. *Biochem. J.* **269**:639–645.
  50. MacPherson, M. R., S. M. Lohmann, and S.-A. Davies. 2004. Analysis of *Drosophila* cGMP-dependent protein kinases and assessment of their in vivo roles by targeted expression in a renal transporting epithelium. *J. Biol. Chem.* **279**:40026–40034.
  51. Majima, T., T. Hamasaki, and T. Arai. 1986. Increase in cellular cyclic GMP level by potassium stimulation and its relation to ciliary orientation in *Paramecium*. *Experientia* **42**:62–64.
  52. Marchler-Bauer, A., J. B. Anderson, C. DeWeese-Scott, N. D. Fedorova, L. Y. Geer, S. He, D. I. Hurwitz, J. D. Jackson, A. R. Jacobs, C. J. Lanczycki, C. A. Liebert, C. Liu, T. Madej, G. H. Marchler, R. Mazumder, A. N. Nikolskaya, A. R. Panchenko, B. S. Rao, B. A. Shoemaker, V. Simonyan, J. S. Song, P. A. Thiessen, S. Vasudevan, Y. Wang, R. A. Yamashita, J. J. Yin, and S. H. Bryant. 2003. CDD: a curated Entrez database of conserved domain alignments. *Nucleic Acids Res.* **31**:383–387.

53. Miglietta, L. A. P., and D. L. Nelson. 1988. A novel cGMP-dependent protein kinase from *Paramecium*. *J. Biol. Chem.* **263**:16096–16105.
54. Müller, S., K. Diederichs, J. Breed, R. Kissmehl, K. Hauser, H. Plattner, and W. Welte. 2001. Crystal structure analysis of the exocytosis-sensitive phosphoprotein, pp63/parafusin (phosphoglucomutase), from *Paramecium* reveals significant conformational variability. *J. Mol. Biol.* **315**:141–153.
55. Murofushi, H. 1974. Protein kinases in *Tetrahymena* cilia. II. Partial purification and characterization of adenosine 3',5'-monophosphate-dependent and guanosine 3',5'-monophosphate-dependent protein kinases. *Biochim. Biophys. Acta* **370**:130–139.
56. Nakaoka, Y., and H. Macheimer. 1990. Effects of cyclic nucleotides and intracellular Ca on voltage-activated ciliary beating in *Paramecium*. *J. Comp. Physiol. A* **166**:401–406.
57. Nelson, D. L. 1995. Preparation of cilia and subciliary fractions from *Paramecium*. *Methods Cell Biol.* **47**:17–24.
58. Orstavik, S., V. Natarajan, K. Tasken, T. Jahnsen, and M. Sandberg. 1997. Characterization of the human gene encoding the type I alpha and type I beta cGMP-dependent protein kinase (PRKG1). *Genomics* **42**:311–318.
59. Pech, L. L. 1995. Regulation of ciliary motility in *Paramecium* by cAMP and cGMP. *Comp. Biochem. Physiol.* **111A**:31–37.
60. Pfeifer, A., P. Ruth, W. Dostmann, M. Sausbier, P. Klatt, and F. Hofmann. 1999. Structure and function of cGMP-dependent protein kinases. *Rev. Physiol. Biochem. Pharmacol.* **135**:105–149.
61. Plattner, H., and N. Klauke. 2001. Calcium in ciliated protozoa: sources, regulation, and calcium regulated functions. *Int. Rev. Cytol.* **201**:115–208.
62. Plattner, H., and R. Kissmehl. 2003. Molecular aspects of membrane trafficking in *Paramecium*. *Int. Rev. Cytol.* **232**:185–216.
63. Plattner, H., and R. Kissmehl. 2005. Molecular aspects of rapid, reversible, Ca<sup>2+</sup>-dependent de-phosphorylation of pp63/parafusin during stimulated exo-endocytosis in *Paramecium* cells. *Cell Calcium* **38**:319–327.
64. Reed, R. B., M. Sandberg, T. Jahnsen, S. Lohmann, S. Francis, and J. Corbin. 1996. Fast and slow cyclic nucleotide-dissociation sites in cAMP-dependent protein kinase are transposed in type Iβ cGMP-dependent protein kinase. *J. Biol. Chem.* **271**:17570–17575.
65. Russell, C. B., D. Fraga, and R. D. Hinrichsen. 1994. Extremely short 20–33 nucleotide introns are the standard length in *Paramecium tetraurelia*. *Nucleic Acids Res.* **22**:1221–1225.
66. Sandberg, M., V. Natarajan, I. Ronander, D. Calderon, U. Walter, S. M. Lohmann, and T. Jahnsen. 1989. Molecular cloning and predicted full-length amino acid sequence of the type I beta isozyme of cGMP-dependent protein kinase from human placenta. Tissue distribution and developmental changes in rat. *FEBS Lett.* **255**:321–329.
67. Schultz, J. E., and S. Klumpp. 1984. Calcium/calmodulin-regulated guanylate cyclases in the ciliary membranes from *Paramecium* and *Tetrahymena*. *Adv. Cyclic Nucleotide Protein Phosphorylation Res.* **17**:275–283.
68. Schultz, J. E., S. Klumpp, and R. D. Hinrichsen. 1990. Calcium and membrane excitation in *Paramecium*, p. 124–150. *In* D. H. O'Day (ed.), Calcium as an intracellular messenger in eukaryotic microbes. American Society for Microbiology, Washington, D.C.
69. Shabb, J. B., and H. D. Corbin. 1992. Cyclic nucleotide-binding domains in proteins having diverse functions. *J. Biol. Chem.* **267**:5723–5726.
70. Smith, J. A., S. H. Francis, K. H. Walsh, S. Kumar, and J. D. Corbin. 1996. Autophosphorylation of type I beta cGMP-dependent protein kinase increases basal activity and enhances allosteric activation by cGMP or cAMP. *J. Biol. Chem.* **271**:20756–20762.
71. Sonneborn, T. M. 1974. *Paramecium aurelia*, p. 469–594. *In* R. C. Kung (ed.), Handbook of genetics, vol. 2. Plenum Press, New York, N.Y.
72. Sperling, L., P. Dessen, M. Zagulski, R. E. Pearlman, A. Migdalski, R. Gromadka, M. Froissard, A. M. Keller, and J. Cohen. 2002. Random sequencing of *Paramecium* somatic DNA. *Eukaryot. Cell* **1**:341–352.
73. Szmidt-Jaworska, A., K. Jaworski, A. Tretyn, and J. Kopcewicz. 2003. Biochemical evidence for a cGMP-regulated protein kinase in *Pharbitis nil*. *Phytochemistry* **63**:635–642.
74. Tischkau, S. A., E. T. Weber, S. M. Abbott, J. W. Mitchell, and M. U. Gillette. 2003. Circadian clock-controlled regulation of cGMP-protein kinase G in the nocturnal domain. *J. Neurosci.* **23**:7543–7550.
75. Treptau, T., R. Kissmehl, J. D. Wissmann, and H. Plattner. 1995. A 63 kDa phosphoprotein undergoing rapid dephosphorylation during exocytosis in *Paramecium* cells shares biochemical characteristics with phosphoglucomutase. *Biochem. J.* **309**:557–567.
76. Uhler, M. D. 1993. Cloning and expression of a novel cyclic GMP-dependent protein kinase from mouse brain. *J. Biol. Chem.* **268**:13586–13591.
77. Vaandrager, A. B., and H. R. De Jonge. 1996. Signalling by cGMP-dependent protein kinases. *Mol. Cell. Biochem.* **157**:23–30.
78. Vaandrager, A. B., E. M. E. Ehlert, T. Jarchau, S. M. Lohmann, and H. R. De Jonge. 1996. N-terminal myristoylation is required for membrane localization of cGMP-dependent protein kinase type II. *J. Biol. Chem.* **271**:7025–7029.
79. Vetter, D., R. Kissmehl, T. Treptau, K. Hauser, J. Kellermann, and H. Plattner. 2003. Molecular identification of a calcium-inhibited catalytic subunit of casein kinase type 2 from *Paramecium tetraurelia*. *Eukaryot. Cell* **2**:1220–1233.
80. Wanner, R., and B. Wurster. 1990. Cyclic GMP-activated protein kinase from *Dicystostelium discoideum*. *Biochim. Biophys. Acta* **1053**:179–184.
81. Weber, I. T., and T. A. Steitz. 1987. Structure of a complex of catabolite gene activator protein and cyclic AMP refined at 2.5 Å resolution. *J. Mol. Biol.* **198**:311–326.
82. Weber, I. T., J. B. Shabb, and H. D. Corbin. 1989. Predicted structures of the cGMP-dependent protein kinase: a key alanine/threonine difference in evolutionary divergence of cAMP and cGMP binding sites. *Biochemistry* **28**:6122–6127.
83. Wernet, W., V. Flockerzi, and F. Hofmann. 1989. The cDNA of the two isoforms of bovine cGMP-dependent protein kinase. *FEBS Lett.* **251**:191–196.
84. Yang, W. Q., C. Braun, H. Plattner, J. Purvee, and J. L. Van Houten. 1997. Cyclic nucleotides in glutamate chemosensory signal transduction of *Paramecium*. *J. Cell Sci.* **110**:2567–2572.
85. Yawo, H. 1999. Involvement of cGMP-dependent protein kinase in adrenergic potentiation of transmitter release from the calyx-type presynaptic terminal. *J. Neurosci.* **19**:5293–5300.
86. Zagulski, M., J. K. Nowak, A. Le Mouel, M. Nowacki, A. Migdalski, R. Gromadka, B. Noel, I. Blanc, P. Dessen, P. Wincker, A. M. Keller, J. Cohen, E. Meyer, and L. Sperling. 2004. High coding density of the largest *Paramecium tetraurelia* somatic chromosome. *Curr. Biol.* **14**:1397–1404.
87. Zieseniss, E., and H. Plattner. 1985. Synchronous exocytosis in *Paramecium* cells involves very rapid ( $\leq 1$  s), reversible dephosphorylation of a 65-kDa phosphoprotein in exocytosis-competent strains. *J. Cell Biol.* **101**:2028–2035.